

Evolution of Galaxy Clustering

J.S.Bagla

Institute of Astronomy, University of Cambridge, Madingley Road, Cambridge CB3 0HA, U.K.

E-mail: jasjeet@ast.cam.ac.uk

2 October 2018

ABSTRACT

We study the evolution of correlation function of dark matter halos in the CDM class of models. We show that the halo correlation function does not evolve in proportion with the correlation function of the underlying mass distribution. Earliest halos to collapse, which correspond to rare peaks in the density field, cluster very strongly. The amplitude of halo correlation function *decreases* from its initial, large, value. This decrease continues till the average peaks have collapsed, after which, the amplitude grows at a slow rate. This behaviour is shown to be generic and the epoch of minimum amplitude depends only on the *rms* fluctuations in mass at the relevant scale and, to a much smaller extent, on the slope of the power spectrum at that scale. We discuss the relevance of this result for interpretation of observations of galaxy and quasar clustering.

Key words: Galaxies : Formation – Cosmology : Theory – Early Universe, Large Scale Structure of the Universe

1 INTRODUCTION

It is believed that structures like galaxies and clusters of galaxies formed by gravitational amplification of small perturbations. This implies that clustering in the mass distribution in the Universe always increases with time. In this model, galaxies form in highly over-dense halos of dark matter. Evolution of galaxy clustering and its relation to the clustering in the underlying mass distribution is an important question that needs to be addressed before we can correctly interpret the observations of galaxy clustering. In this paper we discuss one approach to this problem and comment on the relevance of our results for interpretation of observations of galaxy clustering and its evolution.

Clustering properties of halos have been studied by many authors (See, for example, Gelb and Bertschinger (1994b)). These studies show that there is no simple, scale independent relation between the correlation functions for the mass distribution and halos. Evolution of clustering properties of halos has been studied by Brainerd and Villumsen (1994). They computed the halo-halo correlation function and found that it evolves very slowly in most cases. In some cases they found a *decreasing* phase before the amplitude of the halo correlation function starts growing. Recently, some authors have studied the effects of a decreasing correlation function, and an epoch of minimum amplitude of clustering, on the angular correlation function of galaxies (Ogawa, Roukema and Yamashita 1997).

In this paper we argue that the halo correlation function, for halos above a given mass, has a generic be-

haviour: its amplitude is very large at early times, and decreases very rapidly. The amplitude reaches a minima and then increases at a slow rate.

The paper is organised as follows: §2 outlines a model for evolution of halo clustering. In §3 we describe the numerical simulations used for testing the model. This section also contains details of our approach for identifying halos and calculation of the halo correlation function. Results are presented in §4 and in §5 we discuss the generalisation to galaxy clustering and the relevance of our results for interpretation of observations. We summarise the main conclusions in §6.

2 THE HALO GRAIL

In most models of structure formation, the initial density field is assumed to be a Gaussian random field. Gravitational instability leads to amplification of density perturbations, and over-dense regions collapse to form virialised halos. If the threshold density contrast for formation of halos is much larger than the *rms* dispersion in density contrast, as is the case at early times, only a few rare peaks collapse into halos. These peaks are expected to cluster strongly (Bardeen et. al. 1986) compared to the almost smooth mass distribution, and are poor tracers of the underlying mass distribution. On the other hand, if the threshold is less than, or comparable to, the *rms* dispersion, almost all peaks collapse to form halos and the halo number density traces the mass distribution at scales (much) larger than the typical inter-halo separation. Thus we expect the halos to become “better” tracers of the

arXiv:astro-ph/9711081v2 24 Apr 1998

mass distribution with time. In the following discussion, we quantify these statements and present a simple model for evolution of the halo correlation function.

Consider the distribution of halos of mass M , or larger, before typical halos of this mass have collapsed. To quantify this, we first define a *bias* parameter $\nu(M, z) = \delta_c / \sigma(M, z)$, where $\sigma(M)$ is the (linearly extrapolated) *rms* dispersion in the density contrast at mass scale M and δ_c is the linearly extrapolated density contrast at which halos are expected to collapse and virialise. We use the value $\delta_c = 1.68$, obtained from the spherical top hat collapse model (Gunn and Gott 1972). Most halos of mass M collapse when $\nu(M) \approx 1$. At early times, $\nu \gg 1$, and the number density of collapsed halos is very small (compared to, say, $\bar{\rho}/M$, where $\bar{\rho}$ is the background density at that epoch). We can write the linear correlation function of these rare peaks, at scales where $\frac{\xi(M, r)}{\xi(M, 0)} \ll 1$, as (Bardeen et. al. 1986)

$$\xi_H(M, r) = \exp \left[\nu^2 \frac{\xi(M, r)}{\xi(M, 0)} \right] - 1 \quad (1)$$

Here $\xi(M, r)$ is the correlation function of the smoothed density field (smoothed at mass scale M) evaluated at scale r , and ξ_H is the halo correlation function. The halo correlation has an exponentially large amplitude over the range of scales where $\nu^2 \frac{\xi(M, r)}{\xi(M, 0)} > 1$. At very large scales, the halo correlation function is related to the mass correlation as $\xi_H(M, r) \simeq \nu^2 \frac{\xi(M, r)}{\xi(M, 0)}$. It follows that at early times, characterised by $\nu^2 / \xi(M, 0) > 1$, the halo correlation function has a much larger amplitude than the mass correlation function at all scales.

Time evolution of the linear correlation function for halos, as described in eqn.(1), is controlled by the function ν – the ratio $\frac{\xi(M, r)}{\xi(M, 0)}$ being a function of scale only.

$$\nu(M, z) = \frac{\delta_c}{\sigma(M, z)} = \frac{D_+(z_*)}{D_+(z)} = \frac{1+z}{1+z_*}. \quad (2)$$

Here D_+ is the growing mode for density perturbations in linear theory and z_* is fixed by requiring $\nu(M, z_*) = 1$. The last equality is valid only in the Einstein-deSitter Universe as in that case $D_+(z) \propto (1+z)^{-1}$. D_+ is a monotonically increasing function of time, implying that ν is a monotonically decreasing function. *Therefore, at early times, the amplitude of correlation function of halos is a rapidly decreasing function of time.* In terms of correlation bias,^{*} defined as

$$b^2(r, z) = \frac{\xi_H(r, z)}{\xi(r, z)}, \quad (3)$$

we can say that at early times, bias b increases more rapidly than $(1+z)$ with redshift.

Eqn.(1) gives only the linearly extrapolated correlation function for halos. However, the qualitative behaviour, being exponentially strong, should survive the non-linear evolution.

At later epochs, when $\nu(M) \approx 1$, eqn.(1) is no longer valid. By this time, most halos of mass M have collapsed and the halo distribution begins to trace the underlying mass distribution. Therefore, further evolution of the halo distribu-

tion must reflect the growth of density perturbations. There is another way of explaining this for hierarchical models: low mass halos merge and give rise to more massive halos. As gravity brings halos closer for merger, the halo correlation function must increase. However, the rate of growth of correlation function will be slow as *anti-biased* halos continue to collapse for some time. In other words, the correlation bias will change with redshift at a rate slower than $1+z$.

Thus, there are two effects that contribute to the evolution of correlation function of halos: The *intrinsic* correlation function of halos that have collapsed, and, gravitational instability. These effects act in opposite directions. At early times the rapidly changing *intrinsic* correlation function of the few halos that have collapsed dominates. At late times, gravitational clustering takes over, leading to growth of the correlation function. At some intermediate epoch, these effects must cancel each other leading to a stationary amplitude of the halo correlation function. This is likely to happen when $\nu \approx 1$.

3 NUMERICAL SIMULATIONS

We used a set of simulations of the standard CDM model, normalised so that the linearly extrapolated *rms* fluctuations in density, smoothed with a spherical top hat window function at the scale of $8h^{-1}\text{Mpc}$, is $\sigma_8 = 0.6$. We used $h = 0.5$. All simulations were done with a PM (Particle-Mesh) code and 128^3 particles in a box with the same number of cells.

We used the friends-of-friends (FOF) algorithm with a linking length of 0.3 grid length to identify dense halos. This is larger than the “traditional” value of 0.2 and has been chosen so that the mass function matches the Press-Schechter (Press and Schechter 1975) mass function with $\delta_c = 1.68$. We need to do this to compensate for the lower resolution of a PM code. For the purpose of computing the correlation function, we used halos with 10 or more particles. This was done to avoid noise due to erroneous detections of smaller groups.

In principle, we should identify halos with mass in a given range and compute the correlation function for these at different epochs. However, the following reasons force us to use a different strategy:

- The FOF algorithm is known to link dynamically distinct halos (Gelb and Bertschinger 1994a). (Smaller linking lengths tend to dissolve some halos.) This leads to an incorrect estimate of the mass of halos. We will also underestimate the number of close pairs of halos, and therefore, the amplitude of the correlation function.
- Finite mass resolution in numerical simulations leads to the over-merging problem (Moore, Katz and Lake 1996). The over-merging problem in collisionless simulations makes it difficult to estimate the number of halos of a given mass that may have survived inside bigger halos.

These problems are particularly serious at late times when the number of halos is large and there are many cluster sized halos present in the system. To circumvent these problems we adopt a different approach. We do not consider halos as being one unit each. Instead, we compute the correlation function of particles contained in these halos. This strat-

^{*} Note that this bias is different from ν defined earlier. This degeneracy in nomenclature is unfortunate and we will use the term correlation bias for this one to avoid confusion.

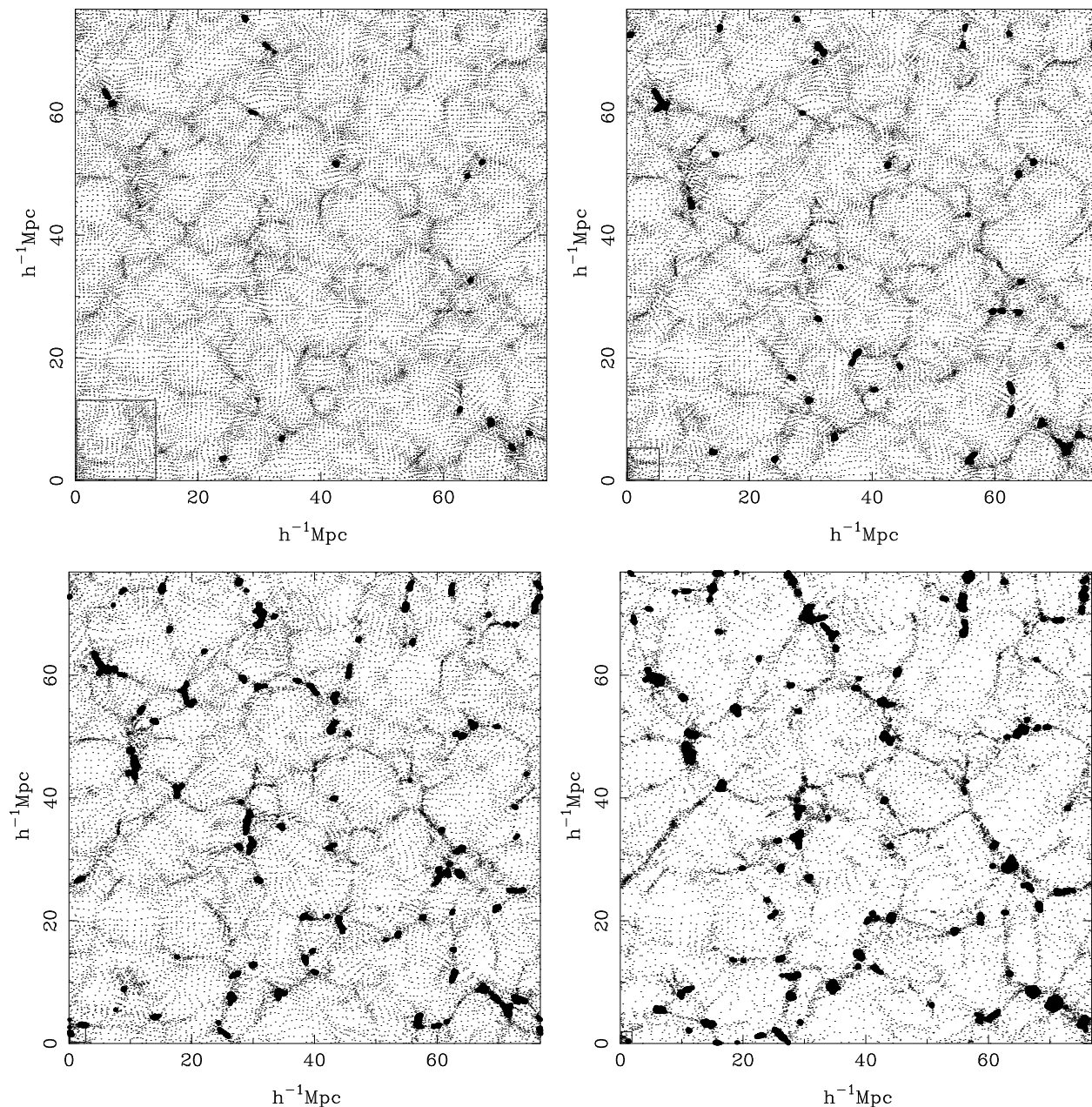


Figure 1. This figure shows the distribution of mass and halos ($M_{halo} \geq 1.2 \cdot 10^{12} M_{\odot}$) in a slice from a CDM simulation. The thickness of the slice is $3h^{-1}\text{Mpc}$. The halo particles are marked as thick points. To highlight the highly non-uniform distribution of halos, we have drawn a box in the lower left corner of each frame that shows the region that should contain one halo if these were distributed uniformly. The upper-left panel shows the slice at $z = 3$, the upper-right panel shows the same at $z = 2$, the lower-left column shows the same slice at $z = 1$ and the lower-right panel is for $z = 0$.

egy is also appropriate for studying the evolution of galaxy correlation function, as galaxies are known to survive inside groups and clusters of galaxies. Although our method ignores the large range in masses of galaxies by using this particular method, we are able to include the contribution of very massive halos that are likely to contain many galaxies.

4 RESULTS

To show that halos cluster very strongly at early times, we have plotted the halos, along with a random subset of all the N-Body particles, in a slice from a CDM simulation with a box size of $76.8h^{-1}\text{Mpc}$. We have shown the same slice at four redshifts; $z = 3, 2, 1$ and 0 . The thickness of the slice is $3h^{-1}\text{Mpc}$ (comoving). The particles in halos ($M_{halo} \geq 1.2 \cdot 10^{12} M_{\odot}$) are shown as thick dots and the N-Body particles are shown as thin dots. A box on the bottom-left corner shows the *projected area per halo*, if the

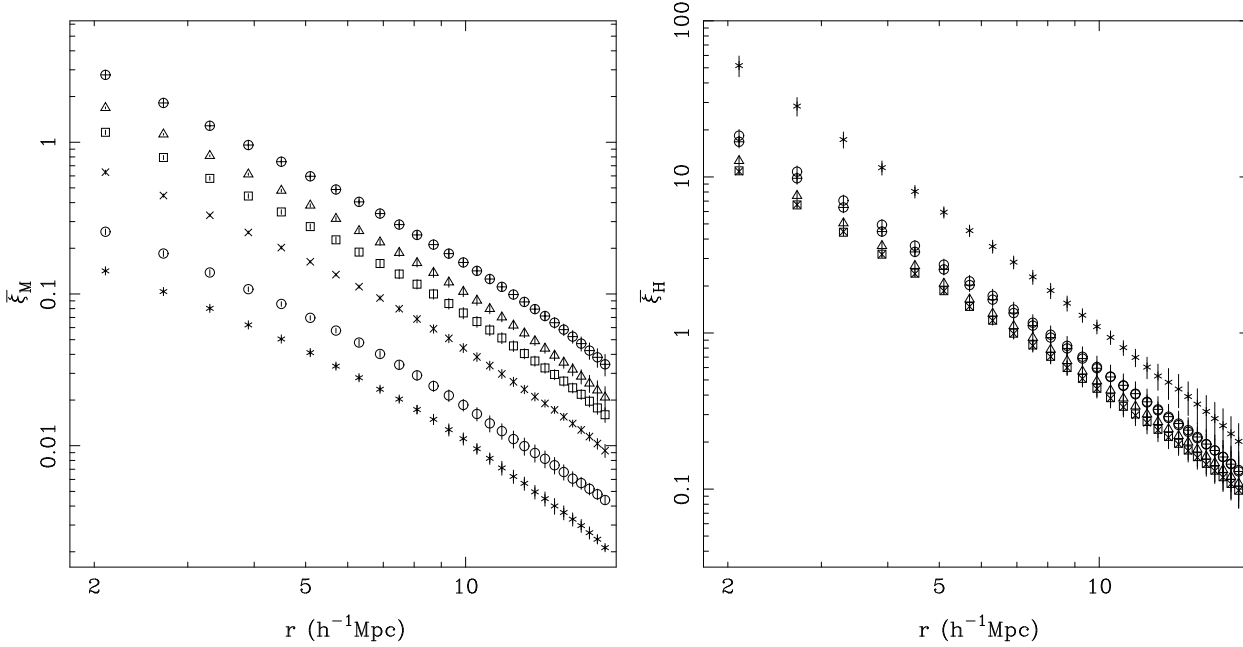


Figure 2. This figure shows the results from simulations of CDM spectrum, like the one shown in fig.1. The averaged correlation function $\bar{\xi}$ is shown as a function of scale $r(h^{-1}\text{Mpc})$. The left panel shows the evolution of clustering in the total mass distribution. As redshift decreases, $\bar{\xi}$ increases monotonically. We have shown the points for $z = 3$ (*), $z = 2$ (○), $z = 1$ (×), $z = 0.5$ (□), $z = 0.25$ (△) and $z = 0$ (⊕). The right panel shows the correlation function of halos with $M_{halo} \geq 1.2 \cdot 10^{12} M_{\odot}$. The amplitude of the halo correlation function decreases rapidly at early times, reaches a minima around $z = 1$ and then increases again. The error bars show the $\pm 1\sigma$ error computed from three realisations of the same power spectrum.

halos were distributed uniformly then there should be one halo in a region of this size on an average. It is clear from this figure that the halo distribution is very non-uniform at early times even though the underlying mass distribution is fairly homogeneous. It is also obvious that the halo distribution develops along the “skeleton” of the late time mass distribution. Halos form along filaments and pancakes, or their intersections. Other simulations also show a similar pattern of evolution. (To see the variation with linking length used for locating halos, see the plots in Brainerd and Villumsen (1994).)

We describe the clustering properties using the averaged two point correlation function $\bar{\xi}(r)$

$$\bar{\xi}(r) = \frac{3}{r^3} \int_0^r x^2 \xi(x) dx = \frac{3J_3(r)}{r^3} \quad (4)$$

where $\xi(x)$ is the two point correlation function. The averaged correlation function is a measure of the excess neighbours around a typical point in a sphere of radius r , whereas the two point correlation function is a measure of excess neighbours in a spherical shell at r .

We have plotted the averaged correlation function for the mass distribution and the halo distribution in fig.2 for simulations like those shown in fig.1. The error bars denote the 2σ dispersion around the mean evaluated using three realisations of the CDM power spectrum. The left panel shows the correlation function for mass and the right panel shows the correlation function for mass contained within halos ($M_{halo} \geq 1.2 \cdot 10^{12} M_{\odot}$). These figures show that the clustering in mass increases monotonically, as expected. These figures also confirm that the amplitude of the halo correlation

function is large at early times and it decreases very rapidly. The amplitude of the halo correlation function reaches a minima at $\nu \approx 1.0$ and then increases again. To show this point more clearly, we have plotted the averaged halo correlation function at two scales as a function of redshift in fig.3. Filled squares show the averaged correlation function at $15h^{-1}\text{Mpc}$ and stars show the averaged correlation function at $5h^{-1}\text{Mpc}$. A dashed line and arrows mark the epoch when $\nu = 1$ for these halos.

The fact that bias is high at early times is an “expected” result that is reflected in all the models for evolution of bias (see below). However, what we are pointing out here with our simple model, that is justified by fig.3, is that the bias evolves faster than $1+z$ at epochs where $\nu \gg 1$ and slower than $1+z$ at epochs where $\nu \ll 1$. This result is contained in the expression for bias derived by Mo and White (1996) but not in the model by Fry (1996).

In simulations of the CDM model with different box size, we find that the amplitude of halo correlation function reaches its minimum at lower ν , i.e. at a later epoch than $\nu = 1$, for more negative indices. We find the range $\nu_{min} = 0.96$ ($n_{eff} = -2.4$) to $\nu_{min} = 1.1$ ($n_{eff} = -1.9$). Here, the index n_{eff} is defined as

$$n_{eff} = -3 + \frac{\partial \ln \sigma^2(r)}{\partial \ln r} \quad (5)$$

where the derivative is evaluated at the mass scale of halos. We are studying the variation of ν_{min} with the index for power law models.

The shape of both the mass correlation and halo correlation changes with time. The halo correlation function becomes less steep with time, whereas the mass correlation

function becomes steeper. If we compare the shape and amplitude of the halo and mass correlation function at $z = 0$ in fig.2 then it is apparent that the halo correlation function has a higher amplitude and it is steeper than the mass correlation function. To quantify this, we have plotted the correlation bias as a function of scale at four redshifts in fig.4. The correlation bias is defined here using the averaged correlation function in the manner of eqn.(3). The left panel shows these for “mass weighted” halo correlation function, i.e. correlation function of mass in halos. The right panel shows bias computed from unweighted halo-halo correlation function. These differ at small scales where the effect of over merging is important. At late times, the lower curve shows strong suppression of bias at small scales due to this effect. However, at early times, this effect is relatively unimportant and the unweighted halo correlation function gives a better estimate of bias. At late times bias computed from the correlation function of mass in halos (left panel) should resemble the galaxy correlation function. The curve corresponding to $z = 0$ shows that bias is a function of scale and it increases at small scales. At large scales it approaches an asymptotic value and does not change much beyond $10h^{-1}\text{Mpc}$.

The qualitative behaviour of the correlation bias as a function of scale does not evolve very strongly. However, at early times the increase in bias at smaller scales is more prominent than at late times. This is a reflection of the change in shape of the matter and halo correlation functions. The scale dependence of correlation bias has important implications for inversion of galaxy power spectrum to obtain the initial power spectrum (see §5.1).

Fig.3 shows the variation of correlation function for halos at two comoving scales ($5h^{-1}\text{Mpc}$ and $15h^{-1}\text{Mpc}$) as a function of redshift. To compare with theoretical models, we first describe the figure in terms of correlation bias. At early times bias varies at a rate faster than $1+z$, the rate of variation is close to $1+z$ at around $\nu = 1$ and then it slows down at lower redshifts. In other words, bias varies very rapidly at early times but at late times the variation is very slow.

The first model we consider assumes that all the halos are assumed to form at the same redshift z_* . These halos form with some initial local bias[†] b_* . The model then evolves the clustering of these halos by solving the continuity equation. For comparison, we have plotted (solid lines) the prediction of this model through the low redshift points. The model predicts

$$b = \frac{z_* + b_*}{1 + z_*} + z \frac{b_* - 1}{1 + z_*} = 1 + (1 + z)(b_0 - 1). \quad (6)$$

b_0 is the bias the $z = 0$. As is clear from this equation, an unbiased set of tracers always remain unbiased. At early times, the combined assumption of conservation of the numbers of halos and a local bias is not valid as the rate of formation of halos is high and these are not fair tracers of the mass distribution – this leads to the strong disagreement of predictions with the simulation data at early times.

[†] Local bias is defined as the ratio between density contrasts in galaxy number and the underlying mass distribution. The model by Fry (1996) assumes that the local bias is independent of position. The assumption of local bias implies a correlation bias that is independent of scale.

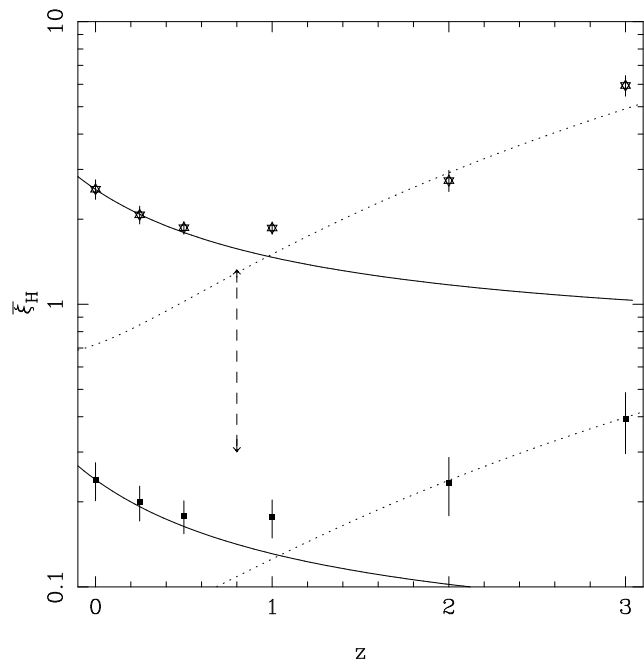


Figure 3. This plot shows the averaged halo correlation function at two scales as a function of redshift. Filled squares show the averaged correlation function at $15h^{-1}\text{Mpc}$ and stars show the averaged correlation function at $5h^{-1}\text{Mpc}$. Error bars depict the $\pm 1\sigma$ dispersion around the mean computed from three realisations of the power spectrum. A dashed line and arrows mark the epoch when $\nu = 1$ for halos of mass $M_{halo} \geq 1.2 \cdot 10^{12} M_{\odot}$. It is clear that the minimum amplitude is reached near that epoch. Thick lines mark the predicted evolution of halo correlation function in the model by Fry (1996). Dotted lines mark the evolution of bias in the model of Mo and White (1996) where we have used the expression for effective bias from Matarrese et al. (1997).

Mo and White (1996) have developed a model for biasing in which the correlation bias is assumed to be independent of scale for halos of any given mass. They predict variation of the form

$$b = 1 + \frac{1}{\delta_c} (\nu^2 - 1) = 1 + \frac{1}{\delta_c} \left\{ \left(\frac{1+z}{1+z_*} \right)^2 - 1 \right\} \quad (7)$$

where the second equality holds only for an Einstein-deSitter Universe.

Matarrese et al. (1997) have generalised the model of Mo and White (1996) by combining the bias for different mass scales. They use many different ansatz for variation of “visibility” of halos and compute the correlation bias in each case. In general, they get the following form for correlation bias

$$b(z) = c_1 + c_2(1+z)^\beta \quad (8)$$

where some of the parameters can be fixed/related by choosing an appropriate ansatz. Using the coefficients for the appropriate $M_{min} = (M_{halo})$ and accounting for the fact that we are using a different normalisation, we have computed the predicted amplitude of correlation function for comparison with the values obtained from simulations. The predictions of their model are shown as dotted lines in fig.3. It is clear that though the match is good at high redshifts, this model does poorly at low redshifts. The main reason being that

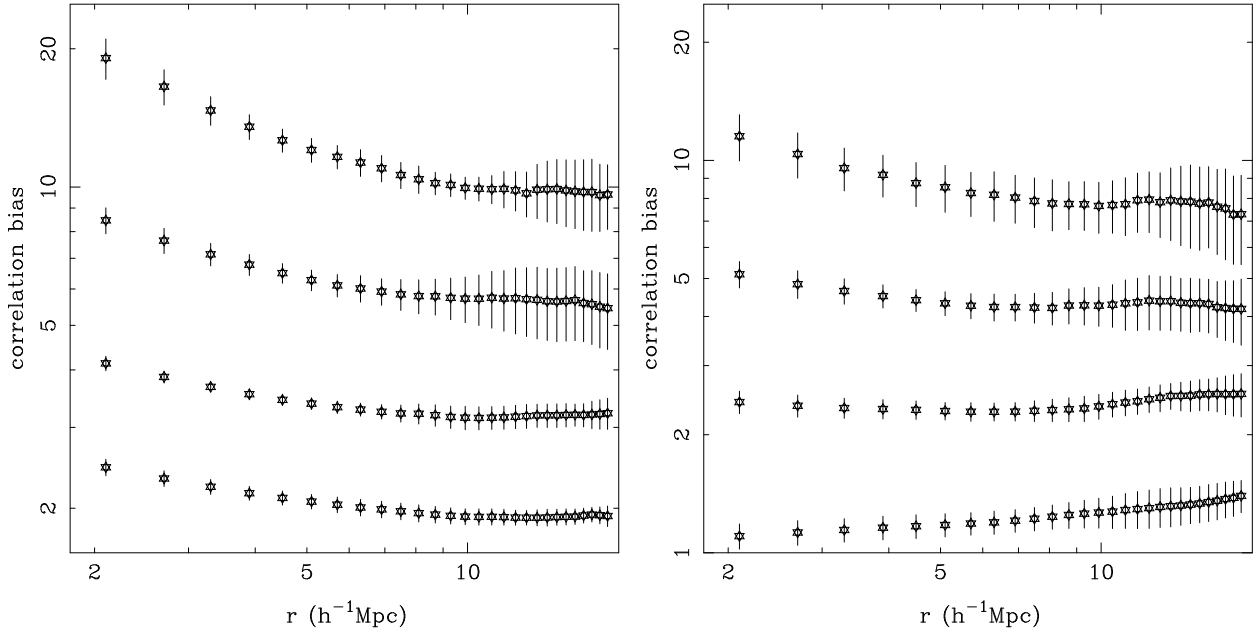


Figure 4. This figure shows correlation bias as a function of scale for four redshifts. This is shown for halos of mass $M_{halo} \geq 1.2 \cdot 10^{12} M_{\odot}$ at $z = 3, 2, 1$ and 0 . Bias decreases monotonically with redshift so the points for $z = 3$ are the ones at the top and the points for $z = 0$ are at the bottom. Error bars depict the $\pm 1\sigma$ dispersion around the mean computed from three realisations of the power spectrum. The left panel shows these for mass weighted halo correlation function. The right panel shows bias computed from unweighted halo-halo correlation function. These differ at small scales where the effect of over merging is important. At late times, the lower curve shows strong suppression of bias at small scales due to this effect.

the parent model, Mo and White (1996), deals with the unweighted halo correlation function. Therefore any comparison with a weighted halo correlation function will not work. However, as we argued in §3, the mass weighted correlation function is a better candidate for the galaxy correlation function. Unweighted halo correlation function predicts an anti-bias at late times. This is never seen in the weighted correlation function and hence the large mismatch.

Some authors have constructed analytical models to understand the evolution of bias (Catelan et al. 1997 and the references cited therein) field where the concept is generalised from statistical bias (only a function of epoch) to a bias that depends both on position and epoch. In these models the mapping from the initial halo distribution to the final one is done using perturbative or approximate methods.

5 DISCUSSION

In §4 we described evolution of the correlation function for mass contained in halos of mass greater than a given cutoff. These results, when applied to galaxies, have many important implications. In §5.1, we will discuss the calculation of the initial power spectrum from the observed galaxy correlation function in view of the results presented in §4. In §5.2 we turn to the question of evolution of galaxy/quasar clustering and its relation with the evolution of halo clustering. Lastly, we outline some implications of these results for evolution of the inter-galactic medium and galaxy formation models in §5.3.

5.1 Galaxy Correlation Function and the Initial Power Spectrum

In this section, we assume that the halo distribution and galaxy distribution are the same at the present epoch. This is a reasonable assumption for studying galaxy clustering at a given epoch, as long as the mass of halos is not too different from the mass of typical galaxies studied in surveys.

The shapes of mass and galaxy correlation functions are different, even at late times (fig.2, fig.3 and fig.4). These differences introduce errors in calculation of the initial power spectrum from observations of galaxy clustering using scaling relations (Peacock and Dodds 1996).

Fig.5 shows the non-linear index n_{nl} as a function of the linear index n_{lin} of the averaged correlation function. We define n_{nl} as in eqn.(5) except that σ^2 is replaced by $\bar{\xi}$. This relation between the indices is obtained by using the power law fit (Bagla and Padmanabhan 1997) in the quasi-linear regime ($1 \leq \bar{\xi} \leq 200$)[‡] to the scaling relation between the linear and the non-linear correlation function (Hamilton et al. 1991). This figure shows that this relation flattens out for indices above $n_{nl} = -1$. Two reasons contribute to this flattening:

- The index $n_{lin} = -1$ is a “critical index” in the sense that power spectra with an index close to $n_{lin} = -1$ change shape so that n_{nl} is closer to this critical index in the quasi-linear regime (Bagla and Padmanabhan 1997).

[‡] For a power law correlation function, $\bar{\xi} = 3\xi/(3 - \gamma)$. Thus for $\gamma = 1.8$, as suggested by observations, this relation between the indices can be used up to about $8h^{-1}$ Mpc.

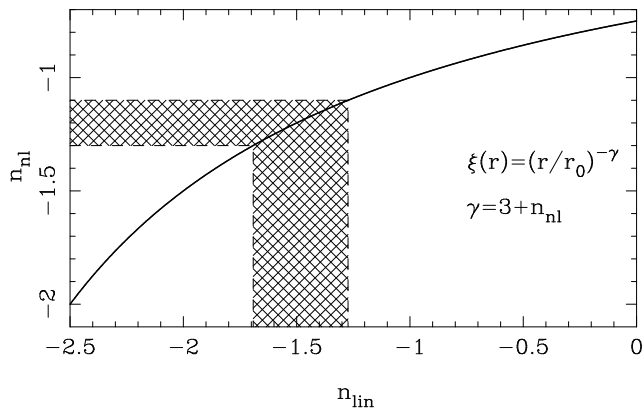


Figure 5. This figure shows the non-linear index of the power spectrum as a function of the linear index in the quasi-linear regime ($1 \leq \bar{\xi} \leq 200$). This relation is derived using a power law fit to the relation between the linear and evolved correlation (Hamilton et al. 1991). We have shown a horizontal shaded region to mark the region $\gamma = 1.8 \pm 0.1$. This translates into a linear index of $\gamma_{lin} \simeq 1.5 \pm 0.2$, marked by the vertical shaded region. This demonstrates the amplification of uncertainty in the index of power spectrum in the inversion process.

- Gravitational clustering of hierarchical models ($n > -3$) restricts the non-linear indices below $n_{nl} \leq 3/\bar{\xi}$ (Bagla and Padmanabhan 1997). In other words, the non-linear index of the power spectrum must be in the range $-3 \geq n_{nl} \geq 0$, irrespective of the initial index.

Gravitational instability acts to decrease (but not to erase) the differences between different initial conditions. Therefore, any uncertainties in the non-linear mass correlation function translate into much larger uncertainties in the initial power spectrum. The difference in the shape/slope and the amplitude of the galaxy correlation function and the mass correlation function is one such uncertainty.

In order to assess this amplification of uncertainty in a quantitative manner, we have mapped a narrow range of non-linear indices, $n_{nl} = -1.2 \pm 0.1$ ($\gamma = 1.8 \pm 0.1$), to the corresponding linear indices. The permitted range of linear indices is much larger ($n_{lin} \simeq -1.5 \pm 0.2$; $\gamma \simeq 1.5 \pm 0.2$). Therefore, even a small error in the non-linear index[§] of the power spectrum can lead to a much larger error in the linear power spectrum. In addition to the uncertainty in slope, uncertainty in amplitude also contributes to the error.

The above discussion shows that inverting the galaxy correlation function to determine the initial power spectrum leads to amplification of uncertainties. This is especially true of scales in the non-linear regime where, in general, correlation bias depends on scale. At larger scales, bias is expected to be scale independent and the main source of error will be the uncertain difference in amplitude.

[§] If we assume the difference between halo clustering and mass clustering to be the only source of error, then we can estimate its magnitude from simulations. The curves for $z = 0$ in fig.2 show this difference to be $\Delta n \simeq 0.2$ for $M_{halo} \geq 1.2 \cdot 10^{12} M_{\odot}$, twice the uncertainty of 0.1 we used in our example.

5.2 Halos and Galaxies

Discussion in this paper has assumed, so far, that galaxy clustering and halo clustering are the same thing. Although this is a reasonable assumption if we are interested in only one epoch with an appropriate choice of minimum halo mass, the same is not true for the relative evolution of the two distributions. Here, we list some plausible alternatives and outline the evolution of galaxy correlation function for each one.

At any given epoch, there are more low mass galaxies than high mass galaxies. This suggests that the galaxy correlation function is dominated by the smallest galaxies[¶]. In such a case, the galaxy correlation function must evolve in a manner similar to the halo correlation function and its amplitude must go through a minimum at some epoch. For low mass galaxies, this minimum could be at $z \gg 0$.

The assumption outlined above applies in a much better way to quasars as these cannot form in very low mass halos and the redshift at which the amplitude of quasar correlation reaches the minima may be low enough to be observable. If the minimum halo mass associated with quasars is greater than $10^{11} M_{\odot}$ then the observed quasar correlation function should have a higher amplitude at $z > 2$ than at $z < 1$. Considering the small probability of a given halo hosting a quasar at a given time, the more appropriate measure for clustering of quasars is provided by the unweighted halo correlation function.

Recent estimates of the quasar correlation function, though based on small datasets, show that clustering of quasars is indeed stronger at higher redshifts (Kundic 1997; La Franca, Andreani and Cristiani 1997). Authors of the second paper claim that the observed evolution of quasar clustering cannot be explained in all models of AGN activity. Our analysis suggests that this need not be true. Quasars must show decreasing clustering amplitude if the AGN activity is not correlated with the large scale environment.

The assumption of a mass threshold also applies very well to groups and clusters of galaxies. Therefore, the cluster correlation function should show a higher amplitude at higher redshifts.

We can use a different ansatz: we can assume that the brightest galaxies reside in halos that have formed relatively recently. We can identify the mass scale $M_*(z)$ by assuming that these correspond to $\nu(M_*) \simeq 1$. For hierarchical models, we know that $\sigma(M_1, z) > \sigma(M_2 > M_1, z)$, implying that $\nu(M_2, z) > \nu(M_1)$. As a high ν corresponds to a high correlation bias, it is clear that the halo correlation function with threshold M_1 will have a lower amplitude than the halo correlation function with threshold M_2 . This indicates that the correlation function of M_* halos at z_1 will have a much lower amplitude than its equivalent at z_2 . Therefore we expect rapid evolution of the galaxy correlation function, much faster than the linear growth rate, if galaxies correspond to M_* halos. This may be a good model for evolution of clustering of faint galaxies (Brainerd, Smail and Mould 1995).

The above discussion shows that the evolution of galaxy clustering is likely to depend strongly on our choice of re-

[¶] There is, of course, the problem of identifying the *same* population of galaxies at different redshifts

lation between halos and galaxies at different redshifts. If we identify similar objects at different redshifts, then these will show either a decreasing correlation function or nearly constant clustering in comoving co-ordinates. On the other hand, if we are working with the most prominent/numerous objects at each redshift then we should see rapid evolution of clustering. Astrophysical effects, in general, make the relation of halos and galaxies a little fuzzy, and this will result in an uncertain linear combination of the two types of evolution of clustering.

Considering the uncertain relation of the relative evolution of galaxy/halo and mass clustering, the rate of growth of the correlation function at large scales should not be interpreted as the linear growth rate of density perturbations. Direct determination of cosmological parameters by assuming the two rates to be identical can lead to wrong results.

5.3 Galaxy Clustering and Reionisation of the IGM

Observations show that the Inter-Galactic Medium (IGM) is ionised at the highest redshifts we can probe using known quasars and galaxies. Scenarios for reionisation of the IGM fall in two basic categories: Ionisation by quasars, which have a low number density and hence the IGM has a very patchy structure at early times. Ionisation by proto-galaxies, dwarf galaxies or star clusters that are distributed uniformly, leading to a quick and homogeneous reionisation.

We have shown in this paper that halos, irrespective of their mass, cluster very strongly at early times. Therefore, the reionisation of the IGM will be patchy at a scale much larger than $n^{-1/3}$, where n is the number density of the sources of ionisation. The non-uniformity of halos at early times is illustrated in fig.1.

It is thought that the earliest clusters of stars formed when low mass halos $M_{halo} \simeq 10^6 M_{\odot}$ collapse after cooling by H_2 line cooling (Tegmark et al. 1997). If these clusters of stars were responsible for reionisation of IGM, then, as these have a very large number density, $n^{-1/3} \approx 10 \text{kpc}_{proper}$, the ionisation structure of the IGM will be fairly homogeneous. However, UV radiation from the first clusters leads to dissociation of H_2 molecules and hence the Jeans mass increases by a considerable amount (Haiman, Rees and Loeb 1997). The second generation of collapsed object are like dwarf galaxies $M_{halo} \simeq 10^{8-9} M_{\odot}$ and these have a slightly lower number density, $n^{-1/3} \approx 0.1 \text{Mpc}_{proper}$. A visual comparison with fig.1 suggests that some parts of the Universe will be at a much greater distance from the nearest source of ionising radiation. Therefore, one may expect patchiness at scales of 1Mpc_{proper} , or about 10Mpc_{comov} . The early stages of reionisation from such sources may be observed using the 21cm tomography type of observations, though at a scale smaller than that suggested for quasars (Madau, Meiksin and Rees 1997). On the other hand, if quasars are responsible for ionising the IGM then the scale of patchiness will be much bigger than that expected from the number density.

The relative distribution of halos and the underlying mass in fig.1 suggests that halos form preferentially along filaments/pancakes or their intersections. Denser filaments and pancakes can “resist” being ionised much more efficiently than the under dense regions. Photo-ionisation in the under-dense region will increase the Jeans mass and suppress

collapse of low mass halos (Efstathiou 1992) at late times. This may be the reason for the apparent lack of dwarf galaxies in voids. This effect will not be as prominent in the filaments as the recombination time is smaller, and, ionisation proceeds much more slowly along over-dense regions than it does in the under-dense regions.

6 CONCLUSIONS

In §5, we have highlighted some implications of the model and simulation results presented in this paper. Our conclusions are summarised below:

- The halo correlation function for halos with mass greater than ($M_{halo} = 1.2 \cdot 10^{12} M_{\odot}$) at $z = 3$ is higher than the correlation function of halos above the same threshold today. Therefore, it is only to be expected that the galaxy correlation function at high redshifts should have a large amplitude (Steidel et al 1998; Bagla 1998).

- The halo correlation function (and the correlation function of mass contained in halos) has a different shape, as compared to the non-linear correlation function of mass. Therefore, inverting the galaxy correlation function to obtain the linear correlation function, or the power spectrum, for mass can lead to wrong answers at small scales ($l \leq 8 h^{-1} \text{Mpc}$).

- The growth rate of correlation function should not be used, directly, to compute ω/λ by assuming linear growth or stable clustering - we have shown that the rate of evolution of halo correlation function has little in common with the matter correlation function, and does not depend in any obvious way on cosmological parameters.

- Quasar correlation function, as it corresponds to high mass halos, should show a decreasing phase at $z > 1$.

- Cluster correlation function should also show a decreasing phase, if we can define a sample of clusters at higher redshifts ($z \simeq 0.5$) with the same mass threshold.

- The rapid evolution of clustering of faint galaxies can be understood if these correspond to M_* galaxies at high redshifts.

- Earliest structures to form in the Universe will cluster strongly, therefore the sources that reionise the Universe will occur in groups that are further apart than expected from their number density and a nearly uniform distribution. This implies that the reionisation will be very patchy and it may be possible to observe the patchiness using the redshifted 21cm radiation (Madau, Meiksin and Rees 1997).

ACKNOWLEDGEMENT

I would like to thank Martin Rees, K.Subramanian, Ofer Lahav and Shiv Sethi for many useful discussions. I acknowledge the support of PPARC fellowship at the Institute of Astronomy.

REFERENCES

- Bagla J.S. and Padmanabhan T. 1997, MNRAS 286, 1023
 Bagla J.S. 1998, MNRAS, In Press

- Bardeen J.M., Bond J.R., Kaiser N. and Szalay A.S. 1986, *ApJ* 304, 15
- Brainerd T.G. and Villumsen J.V. 1994, *ApJ* 431, 477
- Brainerd T.G., Smail I. and Mould J. 1995, *MNRAS* 275, 781
- Catelan P., Lucchin F., Matarrese S. and Porciani C. 1997, *astro-ph/9708067*
- Efstathiou G. 1992, *MNRAS* 256, 43p
- Fry J.N. 1996, *ApJL* 461, 65
- Gelb J.M. and Bertschinger E. 1994a, *ApJ* 436, 467
- Gelb J.M. and Bertschinger E. 1994b, *ApJ* 436, 491
- Gunn J.E. and Gott J.R. 1972, *ApJ* 176, 1
- Haiman Z., Rees M.J. and Loeb A. 1997, *ApJ* 476, 458
- Hamilton A.J.S., Kumar P., Edward Lu and Matthews A. 1991, *ApJL* 374, 1
- Kundic T. 1997, *ApJ* 482, 631
- La Franca F., Andreani P. and Cristiani S. 1997, *astro-ph/9711048*, to appear in *ApJ*
- Madau P., Meiksin A. and Rees M.J. 1997, *ApJ* 475, 429
- Matarrese S., Coles P., Lucchin F. and Moscardini L. 1997, *MNRAS* 286, 115
- Mo H.J. and White S.D.M. 1996, *MNRAS* 282, 347
- Moore B., Katz N. and Lake G. 1996, *ApJ* 457, 455
- Ogawa T., Roukema B.F. and Yamashita K. 1997, *ApJ* 484, 53
- Peacock J.A. and Dodds S.J. 1996, *MNRAS* 280, 19
- Press W.H. and Schechter P. 1975, *ApJ* 187, 452
- Steidel C.C., Adelberger K.L., Dickinson M., Giavalisco M., Pettini M. and Kellogg M. 1998, *ApJ* 492, 428
- Tegmark M., Silk J., Rees M.J., Blanchard A., Abel T. and Palla F. 1997, *ApJ* 474, 1